*applied microbiology*

MDPI

*Article*

# Assessing the Microbial Impact on the Performance of Bentonite Clay at Different Thermo-Hydro-Geochemical Conditions

**Julia Mitzscherling [1,*], Anja M. Schleicher [2,*], Steffi Genderjahn [3], Marie Bonitz [4] and Dirk Wagner [1,5]**

[1] GFZ German Research Centre for Geosciences, Section Geomicrobiology, 14473 Potsdam, Germany; dirk.wagner@gfz-potsdam.de
[2] GFZ German Research Centre for Geosciences, Inorganic and Isotope Geochemistry, 14473 Potsdam, Germany
[3] Helmholtz Open Science Office, 14473 Potsdam, Germany; steffi.genderjahn@os.helmholtz.de
[4] GFZ German Research Centre for Geosciences, Fluid Systems Modelling, 14473 Potsdam, Germany; marie.bonitz@gfz-potsdam.de
[5] Institute of Geosciences, University of Potsdam, 14476 Potsdam, Germany
* Correspondence: julia.mitzscherling@gfz-potsdam.de (J.M.); anja.schleicher@gfz-potsdam.de (A.M.S.); Tel.: +49-331-6264-28886 (J.M.); +49-331-6264-1426 (A.M.S.)

**Abstract:** Because of its swelling capacity, compacted bentonite clay is a suitable buffer material in deep geological repositories for high-level nuclear waste. However, this only applies if the swelling capacity is maintained. Accordingly, bentonites have to be stable to changing temperature, humidity, infiltrating fluids or microbial activity. In batch experiments, we investigated combined microbial and thermo-hydro-geochemical effects on the swelling capacity of uncompacted bentonite MX-80. Bentonite was exposed to fluids of different ionic strength and the bacterium *Stenotrophomonas bentonitica*. Bacterial growth was monitored by counting colony-forming units while the swelling capacity of bentonite was evaluated using in situ XRD at varied temperatures and humidity. The presence of bentonite prolonged the survival of *S. bentonitica*. However, electron microscopy, XRD and ICP-OES analyses showed neither an interaction of *S. bentonitica* with bentonite, nor significant changes in the swelling capacity or element composition. The swelling capacity and diffraction peak intensity were, however, strongly reduced by the ionic strength of the fluid and the exposure time. The study highlights that bentonite is affected by thermo-hydro-geochemical and microbial processes to different degrees and that the complexity of different co-occurring factors in potential nuclear waste repositories is important to consider in safety assessments.

**Keywords:** bentonite; swelling; MX-80; thermo-hydro-chemical behaviour; *Stenotrophomonas bentonitica*; engineered barrier; deep geological repository; nuclear waste



**Citation:** Mitzscherling, J.; Schleicher, A.M.; Genderjahn, S.; Bonitz, M.; Wagner, D. Assessing the Microbial Impact on the Performance of Bentonite Clay at Different Thermo-Hydro-Geochemical Conditions. *Appl. Microbiol.* **2024**, *4*, 1091–1109. https://doi.org/10.3390/applmicrobiol4030074

Academic Editor: Ian Connerton

Received: 4 June 2024
Revised: 15 July 2024
Accepted: 16 July 2024
Published: 20 July 2024



## 1. Introduction

As part of a multibarrier system, clay is an important material in many deep geological repository (DGR) designs for high-level nuclear waste (HLW) [1,2]. Besides being considered as host rock, highly compacted bentonite-based clay is the primary candidate for buffer material because of a high sorption capacity for radionuclides [3,4], a favourable swelling ability that enables sealing through a high swelling pressure [5], and low water activity that has been demonstrated to suppress microbial growth [6]. Nevertheless, bentonites are suitable materials for the production of geotechnical barriers only if the swelling capacity is maintained at the conditions expected. Accordingly, bentonites have to be stable with respect to changing temperature and humidity, as well as the possible impact of infiltrating fluids and/or microorganisms.

The effect of temperature on the hydro-mechanical response of bentonite engineered barriers is one important aspect in a DGR after placing the high-level nuclear waste into the repository. Depending on the DGR concept, peak temperatures at the canister-bentonite interface can reach 80 to 160 °C [7,8]. Such heating reduces the swelling and adsorption

capacity in bentonite clay by neutralising permanent charges. The main clay mineral in bentonite is montmorillonite (a smectite), which is characterised by a layered structure of tetrahedral and octahedral sheets and a negative charge. Heating can cause small cations to migrate through the tetrahedral sheet into the octahedral vacancies of the 2:1 layer [9–11]—a mechanism which can lead to smectite degradation.

The properties of the exchangeable cations in bentonite, such as charge, hydration energy and size affect the ability of adsorption and attenuation of water significantly [12]. The salinity of infiltrating solutions can also conceivably impact the structure of bentonite due to cation exchange reactions, dissolution and precipitation, or recrystallisation processes (e.g., [13–18]). Portland cement pore waters from the technical barrier, for instance, are $Ca^{2+}$-rich and alkaline [19], while formation waters in clay or crystalline host rocks are often dominated by NaCl at moderate pH [20,21]. In particular, the presence of cations with higher valences, i.e., a higher charge density in the interlayer, decreases the swelling capacity of bentonite [22]. Upon reaction with NaCl solutions, some studies report on changes in the bentonite properties such as the dissolution of smectite and formation of other minerals [14], a decrease in the cation exchange capacity [15,16,18,23], a reduction in swelling and XRD (X-ray diffraction) reflection broadening with increasing time [24], or asymmetry and reflection shifting to lower *d*-values due to hydration heterogeneities [25]. However, Kaufhold et al. [26] only observed cation exchange but no structural changes in NaCl solutions of moderate pH up to 60 °C.

Microorganisms have been detected in natural bentonite horizons [27], despite the inhospitable conditions in clay formations such as low porosity [28], low water availability [29] and a lack of easily accessible and easily degradable energy sources [30,31]. Physico-chemical changes caused by the construction and operation of the DGR could stimulate these indigenous microorganisms. In addition, foreign microorganisms can be introduced by the intrusion of water along fractures or during the construction of the DGR. Microbial activity is predicted to occur at less densely packed interfacial environments and areas of disturbance, such as fractures and faults, where the bentonite barrier is disrupted, at least temporarily [6]. In those environments, the physical conditions necessary to suppress microbial activity are not always met. Microbial activity in the immediate vicinity of waste containers or in the near-field (including the engineered barriers and parts of the host rock in contact with the engineered barriers) may result in the corrosion of the containers, microbial gas production, the dissolution of clay minerals or leaching of specific elements from those minerals. On the other hand, microorganisms can adsorb radionuclides or mediate the reduction in gas pressure build-up, reducing the volume of gas [32]. The microbial gas production can reduce the effectiveness of the bentonite-based barriers and/or natural barriers. The microbial adsorption of radionuclides can either result in their immobilisation in biofilms or their enhanced migration through fractures by microbes acting as colloids. However, apart from the exchange of interlayer cations, leaching and dissolution of the clay minerals by microbial activity may also retard mineral attack in a various ways or promote mineral growth [33–36]. Whether microorganisms promote mineral alteration or protect minerals depends on the system [37].

The complex interaction of minerals, solutions and bacteria has gained increasing attention since any reaction that leads to the reduction in the swelling capacity of smectite and thus to a loss of safety of the waste container is of relevance. At present, it is not well understood how different microorganisms may affect the clay mineral smectite when in contact with different aqueous solutions. Numerous studies investigated the swelling behaviour of bentonite clays in contact with different saline or alkaline solutions of simple composition (e.g., [19,26,38–40]). However, the swelling in mixed salt solutions, as can be found in groundwaters of surrounding host rocks which are blended with a variety of chemical components, is poorly studied [22].

The present study aimed to investigate the combined microbial and thermo-hydro-geochemical effects on the swelling capacity of uncompacted bentonite MX-80 when ex-

posed to fluids of different ionic strength and the bentonite-dwelling bacterium *Stenotrophomonas bentonitica* BII-R7$^T$.

## 2. Materials and Methods

### *2.1. MX-80 Wyoming Bentonite*

The bentonite used in this study is a Wyoming bentonite MX-80 (Na-montmorillonite), obtained from American Colloid Company (Volclay MX-80, Wyoming clay, lot number 17912; Figure 1a, Hoffman Estates, IL, USA). MX-80 bentonite is composed of ~76% of montmorillonite (smectite) and the accessory minerals mica (2.8–3.8%), feldspar (4.5%), quartz (5–6%), calcite (0.3–0.4%) and pyrite (0.5%) [41,42].

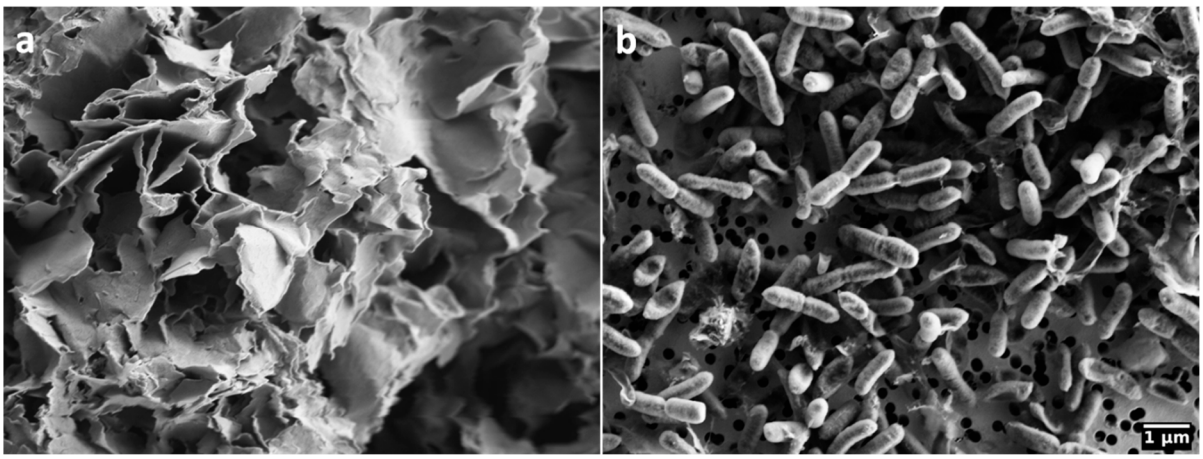


**Figure 1.** Scanning electron microscopy images of (**a**) Wyoming bentonite MX80; (**b**) Gram-negative, facultative anaerobic bacterium *Stenotrophomonas bentonitica* BII-R7$^T$.

The bentonite was sterilised via electron beam irradiation (10 mEV, 30 kGy) using the STERIS Herotron E-Beam Service GmBH (Bitterfeld-Wolfen, Germany). Sterilisation slightly increased the intensity of the (001) montmorillonite peak (Figure S1). The sterilised MX-80 was stored in autoclave sterilised containers and handled aseptically throughout all experiments.

### *2.2. Stenotrophomonas Bentonitica BII-R7$^T$*

The type strain used in this study was *Stenotrophomonas bentonitica* BII-R7$^T$ (DSM 103927). It was obtained from the German Collection of Microorganisms and Cell Cultures GmbH (DSMZ, Braunschweig, Germany). The purity of the strain was verified using 16S rRNA gene sequencing.

*Stenotrophomonas bentonitica* BII-R7$^T$ (Figure 1b) was originally isolated from bentonite formations in southern Spain (Cabo de Gata, Almeria, Spain) [43]. It is a facultative anaerobic bacterium that is able to grow at temperatures between 15 and 37 °C, with a growth optimum at 28 °C and an optimal pH of 7. It is also able to grow on NaCl concentrations of up to 5% [44].

This particular species was chosen as a model organism for the present study on MX-80 bentonite, as it occurs in natural bentonite formations, which are an excellent and suitable reference material of engineered barriers in DGRs for nuclear waste storage. Besides aerobic respiration, *S. bentonitica* is able to reduce nitrate to nitrite, indicating that anaerobic growth is also possible [44]. Based on its origin and lifestyle, we assume that *S. bentonitica* has the ability to actively grow in and on bentonite clays. Furthermore, *S. bentonitica* BII-R7$^T$ was shown to influence the chemical speciation and mobility of radionuclides such as selenite ($Se^{IV}$) and uranium ($U^{VI}$) [43,45] as well as europium ($Eu^{III}$) and curium ($Cm^{III}$) [46].

### *2.3. Experimental Solutions and Growth Media*

Prior to experimentation, *S. bentonitica* was incubated in Standard Nutrient Broth I, whereas plate count testing was performed on Standard Nutrient agar I (Carl Roth GmbH, Karlsruhe, Germany).

Batch experiments were performed in three differently composed aqueous solutions covering a range of salinities (ionic strengths 0–0.38 M): (i) MilliQ water ($H_2O$), which was used as a control solution and results in the formation of bentonite pore water, (ii) 0.9% NaCl solution (hereafter NaCl), which is a physiological salt solution and mimics formation waters in clay or crystalline rocks, (iii) artificial Opalinus Clay porewater (hereafter OPW), which is the pore water composition of the argillaceous formation Opalinus Clay at Mont Terri Rock Laboratory in Switzerland (composed of 212 mM NaCl, 26 mM $CaCl_2$, 14 mM $Na_2SO_4$, 1.6 mM KCl, 17 mM $MgCl_2$, 0.51 mM $SrCl_2$ and 0.47 mM $NaHCO_3$) [47,48]. All solutions were prepared in autoclave sterilised MilliQ water and were finally filter sterilised (0.2 µm, Whatman Membrane Filter, GE Healthcare Life Sciences, Chicago, IL, USA). Due to contamination, the results obtained with $H_2O$ were excluded from the study. These (Result S1, S2) and other additional figures can be examined in the Supplementary Materials, and raw data are available in the GFZ data publication [49].

Each of the solutions were amended with acetate as the carbon source. We used an acetate concentration of 200 µM according to the concentration in Opalinus Clay pore water found at the Mont Terri rock lab [50]. In order to provide a nitrogen source, we added $NH_4Cl$ at a final concentration of 2 g $L^{-1}$ to a set of the batch cultures prior to inoculation. The stock solution of $NH_4Cl$ was prepared separately and filter sterilised.

#### 2.3.1. Batch Solution Experiments

Before inoculating the mesocosms, *S. bentonitica* was grown in Standard Nutrient Broth I for 24 h. Cells were harvested in the exponential growth phase and washed in the respective solution used for the experiment (3 washings using centrifugation at 8000× *g* for 10 min). Cell density was determined with a Neubauer chamber (depth 0.005 mm) using a magnification of 40. Microscopy was performed with a Leica DM2000 microscope (Leica Camera AG, Wetzlar, Germany).

For each condition, we prepared one mesocosm with 3 g of sterilised MX-80 that was dispensed in 100 mL aqueous solution in 300 mL Erlenmeyer culture flasks. Suspensions were inoculated with the washed bacterial cultures at a starting cell density of $10^5$ cells $mL^{-1}$. Negative controls were not inoculated with bacterial cells and positive controls contained bacterial cells but no MX-80 bentonite. Mesocosms were incubated for at least 61 days at 28 °C under continuous agitation at 50 rpm.

#### 2.3.2. Plate Count Testing

Cell density in the batch cultures was monitored over the course of the experiment using plate count testing. It was expressed as colony-forming units (CFU) per ml. According to the procedure of Miles et al. [51], we diluted slurry samples using serial dilution (1:$10^1$–1:$10^8$) and applied a volume of 20 µL of each dilution in triplicates to agar plates. Prior to sampling, sedimented bentonite was resuspended using vigorous shaking in order to obtain a homogenous suspension.

The purity of *S. bentonitica* in the mesocosms was assessed regularly using a visual control of the colony morphology on agar plates during plate count testing. Thus, important results on mineralogical properties in NaCl and OPW were obtained with pure cultures of *S. bentonitica*.

#### 2.3.3. In Situ X-ray Diffraction Analysis

After 2, 5, 15, 35 and 61 days of incubation, we sampled the mesocosms for the X-ray diffraction analysis (XRD) of bentonite. A volume of 150 µL of the experimental slurry was applied to a glass slide and air dried at room temperature in a laminar flow box overnight. The glass slide was mounted in a humidity chamber attached to a PANalytical Empyrean

X-ray diffraction device with CuK$\alpha$ radiation, automatic divergent and anti-scatter slits, and a PIXel3D detector. The data were recorded from 2 to 50 °2theta via continuous scan with a step size of 0.00131 °2theta and a scan time of 120 s per step for generator settings of 40 kV and 40 mA.

To evaluate the effects of humidity and temperature on the swelling behaviour of the bentonite after interaction with bacteria and solutions, we used a gas-flushed humidity chamber ("CHC plus" Cryo & Humidity chamber, Anton Paar GmbH, Tokyo, Japan) attached to the XRD instrument. The reaction chamber was equipped with a "TCU 110" temperature control unit, designed to control the temperature directly at the sample holder. A controlled gas flow rate and regulated humidity was achieved using a temperature/humidity sensor placed within the chamber. XRD analyses were performed at different temperatures (27 °C, 55 °C, 80 °C) and relative humidity (RH = 0, 50, 80%). When the sample holder was mounted to the stage, the chamber was closed and flushed with dry gas at the certain temperature, until the relative humidity kept at constant values of about 2 ($\pm$0.5) % RH. All XRD measurements were performed at these conditions.

#### 2.3.4. Washing of Bentonite

In order to test whether the removal of salty solutions result in the restoration of the swelling capacity, the MX-80 bentonite was treated as follows: 2 mL of the batch cultures with and without bacteria in NaCl and OPW were centrifuged at 10,300$\times$ *g* for 5 min. The supernatant was discarded and 2 mL of MilliQ was added. The clay pellet was resuspended using vigorous shaking for 5 to 10 min and centrifuged again. The procedure was repeated three times. Finally, 150 µL of resuspended clay samples were mounted onto a glass slide and analysed using XRD.

#### 2.3.5. Ion Chromatography Analysis (Acetate Concentration)

The acetate concentration in all mesocosms in comparison to the initial concentration was determined after 29 days of incubation. An aliquot of 2 mL was sedimented at 17,000$\times$ *g* for 5 min. The supernatant was filtered through Minisart® Syringe Filters (0.22 µm polyether sulfone, Sartorius, Göttingen, Germany) and the acetate concentration was determined via ion chromatography (ICS 3000 Ion Chromatography System, Thermo Fisher Scientific, Waltham, MA, USA), using a Dionex™ OnGuard™ II AG/H cartridge (EMD Millipore, Billerica, MA, USA) to remove chloride, an As11-HC column (Ag11-HC precolumn) and a conductivity detector. The eluent was a gradient of KOH solution. The flow rate was set to 0.38 mL min$^{-1}$. The column oven temperature was 15 °C and 10 µL of the sample was injected into the eluent stream.

#### 2.3.6. Electron Microscopy Analysis

SEM imaging was performed with a Zeiss Merlin VP Compact (Carl Zeiss Microscopy, Oberkochen, Germany) field emission scanning electron microscope at UFZ Leipzig. In order to be sufficiently surface sensitive and at the same time achieve a lateral resolution better than 5 nm, the electron acceleration voltage was set to 2 kV and a 30 µm aperture. The resulting beam current amounted to about 250 pA. The images were acquired in secondary electron detection mode using an Everhard–Thornley type detector. In order to improve the signal-to-noise ratio 10 times, line averaging was employed for the acquisition.

#### 2.3.7. ICP-OES Chemical Analysis

In order to analyse the elemental composition of the clay as well as of the fluids, after 7, 15, 35 and 61 days of incubation, an aliquot of 5 mL of each experimental solution containing bentonite was centrifuged at 20,000$\times$ *g* for 15 min. The supernatant was filtered through Minisart® Syringe Filters (0.22 µm, polyether sulfone filter, Sartorius, Göttingen, Germany) to obtain a 2–3 mL of solution. The bentonite pellet was dried at 50 °C for several days. The major elemental composition was analysed using inductively coupled plasma-optical emission spectrometry (ICP-OES) using an Agilent 5110 ICP-OES instrument (Santa

Clara, CA, USA). The analytical precision and reproducibility are generally better than 2%, regularly tested using certified reference material and in-house standards.

The pH of the fluids was analysed in duplicates or triplicates with the pocket meter LAQUAtwin pH-11 (Horiba scientific, Piscataway, NJ, USA).

### *2.4. Statistics*

For statistical analyses of the X-ray diffraction patterns, we used the measured intensity values at *d*-values ranging from 0 to 11 °2theta covering the range of the Montmorillonite peak at 001. Analyses were performed with the software Past 4.01 [52]. Canonical correspondence analysis (CCA) was used to assess the variation in peak intensity and *d*-values caused by incubation time, ionic strength of the solution, relative humidity and temperature. These factors, as well as the bacterial counts, were fitted into the ordination plot. Triplots shown in the CCA had a scaling type of 0.5. Factors contributing to changes in the peak intensity and location were determined using Mantel tests. Prior to testing, the factors were standardised using z-score transformation. The influence of bacteria on the swelling capacity, i.e., the smectite peak intensity and *d*-spacing, was assessed using a permutational approach of a multivariate analysis of variance (PerMANOVA).

The ionic strength of each experimental solution was calculated according to the composition and concentration of amendments before being in contact with bentonite. We quantified the molar ionic strength *I*, which is a function of the concentration of all ions present in a solution, by applying the following formula [53]:

$$I = \frac{1}{2}\sum_{i=1}^{n} c_i z_i^2$$

where $c_i$ is the molar concentration of ion $i$ (in M, mol/L) and $z_i$ is the charge of that ion.

## 3. Results

### *3.1. Bacterial Growth with Bentonite*

The cell abundance of *S. bentonitica* in the mesocosms was determined over a period of 63 days. In NaCl solution with MX-80 bentonite, the number of CFU slowly but steadily decreased from $8 \times 10^4$ mL$^{-1}$ to 1 within 55 days (Figure 2a). By contrast, the number of CFU in NaCl without MX-80 bentonite rapidly decreased from almost $10^4$ CFU mL$^{-1}$ after inoculation to 0 after 2 days of incubation.

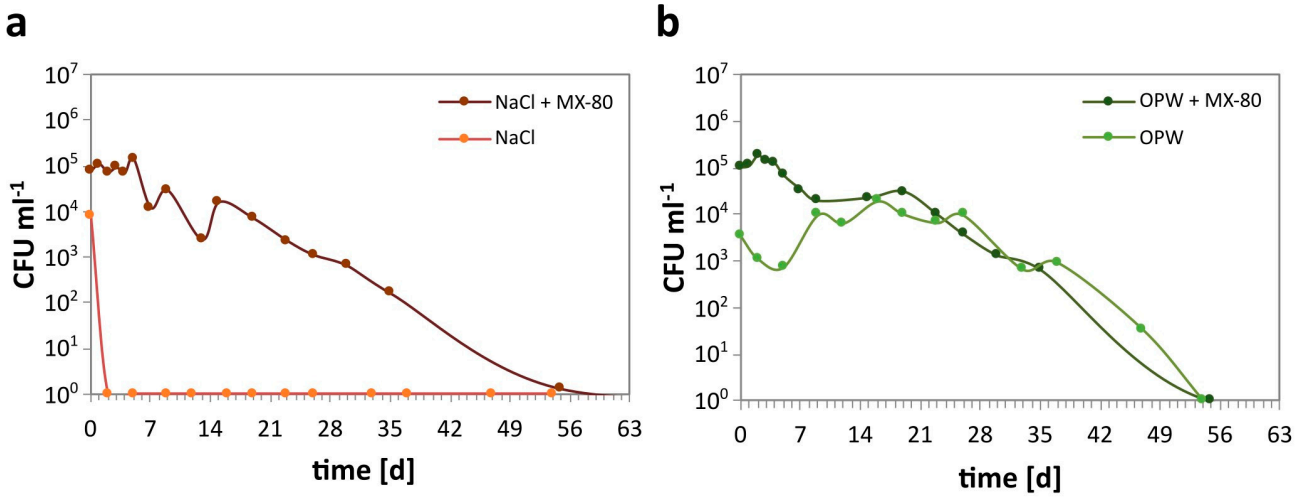


**Figure 2.** Growth of *S. bentonitica* determined as CFU mL$^{-1}$ in solutions of different composition with MX-80 (+MX-80) and without the addition of MX-80 bentonite. (**a**) CFU abundance in NaCl, and (**b**) CFU abundance in OPW.

Similar to NaCl, the CFU number in OPW with MX-80 bentonite steadily decreased from $10^5$ to 0 within 55 days (Figure 2b). Contrary to the NaCl mesocosms without MX-80, the CFU in OPW without MX-80 initially decreased within 5 days to below $10^3$ CFU $mL^{-1}$ but increased again to $10^4$ $mL^{-1}$ after 9 days. The CFU abundance remained more or less stable at $10^4$ $mL^{-1}$ until 26 days of incubation. This was followed by a decrease down to 0 after 54 days, similar to OPW with MX-80.

#### 3.1.1. Swelling Capacity of MX-80 Bentonite with/without *S. bentonitica*

In order to investigate whether the presence of *S. bentonitica* affects the swelling capacity of MX-80 bentonite, the material dispersed in the aqueous solutions was analysed with the humidity/temperature chamber connected to the XRD. Despite the presence of *S. bentonitica* for 54 days in NaCl and OPW, significant differences in peak positions due to the intake of aqueous solution into the interlayer sheets were not observed (Figure 3). In fact, with and without the occurrence of bacteria, the *d*-values of the $d_{001}$ montmorillonite peaks correlated well, and at all temperatures and humidities investigated, the $d_{001}$ peak positions showed a similar shift in presence of *S. bentonitica* compared to bacteria-free bentonite (Table S1). The occurrence of *S. bentonitica* did not significantly influence the swelling behaviour at all different temperatures and humidities after 61 days in all solutions, as confirmed by a pairwise permutational MANOVA (Table S2).

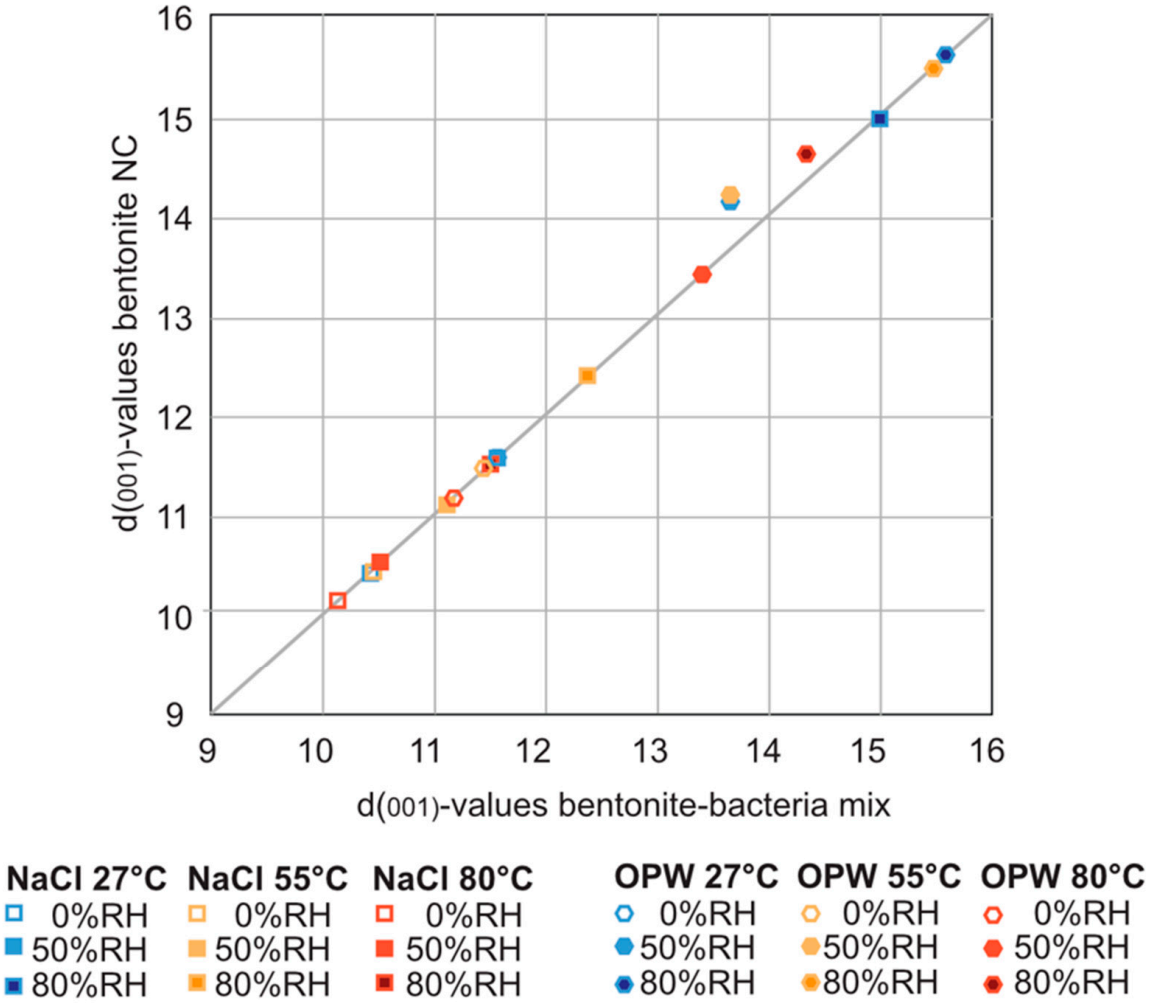


**Figure 3.** Correlation curve of d(001)-values of montmorillonite with (x-axis) and without bacteria (y-axis) in NaCl, and OPW solutions at different temperatures and humidities (see also Table S1).

3.1.2. In Situ Temperature, Humidity, and Salinity Changes in the Presence of *S. bentonitica*

In order to confine the temperature and humidity range of a HLW repository, we focused on the swelling capacity of MX-80 bentonite at 0, 50 and 80% RH, and at 27 °C, 55 °C and 80 °C (Figure 4). This is important, because at temperatures of 80 °C and higher, mineral transformations can occur that lead to a loss of the swelling and sorption capacity [54–57]. Depending on the DGR concept and simulation, 80 °C is at the lower range of maximum temperatures to be expected in the vicinity of the spent fuel container [7,8,58].

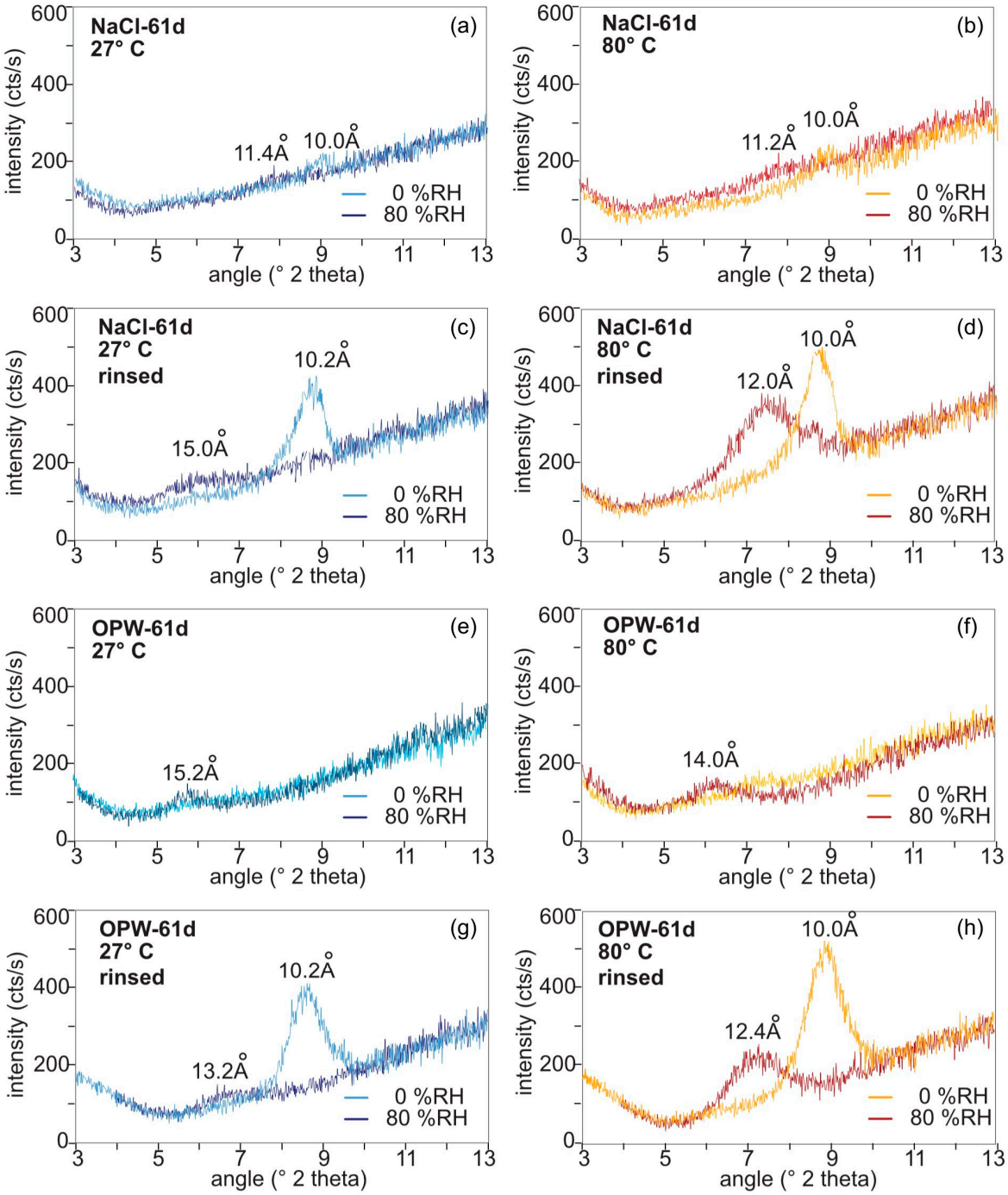


**Figure 4.** XRD spectra of MX-80 after 61 days of exposure to *S. bentonitica* in NaCl and OPW determined at 27 °C (left panel) and 80 °C (right panel) at 0% and 80% relative humidity. (**a**,**b**), in NaCl, (**c**,**d**) after washing off the NaCl solution, (**e**,**f**) in OPW, (**g**,**h**) after washing off the OPW solution.

The impact of salinity on the swelling capacity of bentonite was evaluated by dispersing MX-80 bentonite in solutions of different ionic strength. The calculated ionic strength *I* of the solutions was lower in NaCl solution (*I* = 0.1542) and higher in OPW (*I* = 0.3868, Table S3). Changes in the *d*-spacing of montmorillonite in the bentonite were investigated after 2, 35 and 61 days exposure to the respective solution. When incubating the bentonite with *S. bentonitica* in NaCl (Figure 4a–d) and OPW (Figure 4e–h) for 61 days, the intensity of the 001 peak drastically decreased in the salty solutions over time (Figure S2) and, thus, peak shifts were difficult to evaluate. While the montmorillonite peak 001 was absent in the OPW solution, in NaCl the intensity was reduced after 2 d and it further decreased with incubation time in NaCl (Figure S2; Figure 4a,b,e,f). Therefore, in order to analyse the swelling capacity after having contact to salty solutions, the bentonite was rinsed with water and analysed again (Figure 4c,d,g,h).

The NaCl-saturated samples at 27 °C showed a shift of the $d_{001}$ value from 10.2 Å (8.7 °2theta) at 0% RH to 15.0 Å (5.9 °2theta) at 80% RH (ca. 15 wt% water; Figure 4c). At 80 °C, a shift from 10 Å (8.8 °2theta) at 0% RH to 12.0 Å (7.35 °2theta) at 80% RH (ca. 7 wt% water; Figure 4d) was recognised. This reflects a loss of interlayer water to a minimum of 9 wt%. After incubating bentonite in OPW for 61 days, the water intake into the smectite interlayers was reduced in comparison to NaCl (Figure 4g,h). At 27 °C, the $d_{001}$ value shifted from 10.2 Å (8.7 °2theta) at 0% RH to 13.2 Å (6.7 °2theta) at 80% RH (ca. 10 wt% water; Figure 4g). At 80 °C, the d-value shift ranged from $d_{001}$ 10.0 Å at 0% RH and 12.4 Å (7.25 °2theta) at 80% RH (ca. 8.7 wt% water; Figure 4h).

In order to analyse the multidimensional effect of ionic strength (salinity), time, humidity and temperature on the swelling behaviour of MX-80, the diffractograms were visualised in a CCA ordination (Figure 5). Together, both axes of the CCA explained more than 88% of the variance of sample points, representing single diffractograms (*d*-values ranging from 2 to 11 °2theta). The length of the vectors indicate that time and temperature had the greatest influence on the variance along the x-axis, and thus the greatest impact in general, since the x-axis explained >62% of the variation. Ionic strength and humidity explained >25% of the variance along the y-axis.

Ionic strength was responsible for the separation of NaCl and OPW samples along the y-axis, while humidity caused the variance within each sample cluster. The NaCl sample clusters with the lower ionic strength were located on the bottom left of the plot, while OPW sample clusters with elevated ionic strength were placed to the top right side of the plot. Time separated sample clusters along the x-axis and increasing time resulted in a shift of sample clusters to the right side of the plot. Temperature caused the variance of samples within each sample cluster along the x-axis.

In accordance with increasing ionic strength and time MX-80 remained in the respective solution, the variance within a cluster along the y-axis decreased as the intensity of the montmorillonite peaks decreased.

According to a Mantel test, the factors of ionic strength, time, temperature and humidity altogether significantly correlated with the diffractograms ($p$ = 0.0001, R = 0.48). Mantel tests of the single factors revealed that time ($p$ = 0.0001), ionic strength ($p$ = 0.0015) and temperature ($p$ = 0.0130) correlated significantly, with time having the greatest impact (R = 0.65) on the diffractograms of MX-80 bentonite, including peak shift and height (Table S4). According to the diffractograms (Figure S2), the decreasing variance of clusters along the y-axis observed in the CCA could be explained by generally lower intensities and smaller shifts of the montmorillonite peak. The decreasing peak intensities and d-spacings were caused by time bentonite remained in a solution. Within single clusters the variance, i.e., the swelling capacity at a certain time point, was mainly explained by temperature on the x-axis and by humidity along the y-axis, although humidity had no significant impact on the diffractograms on an overall level.

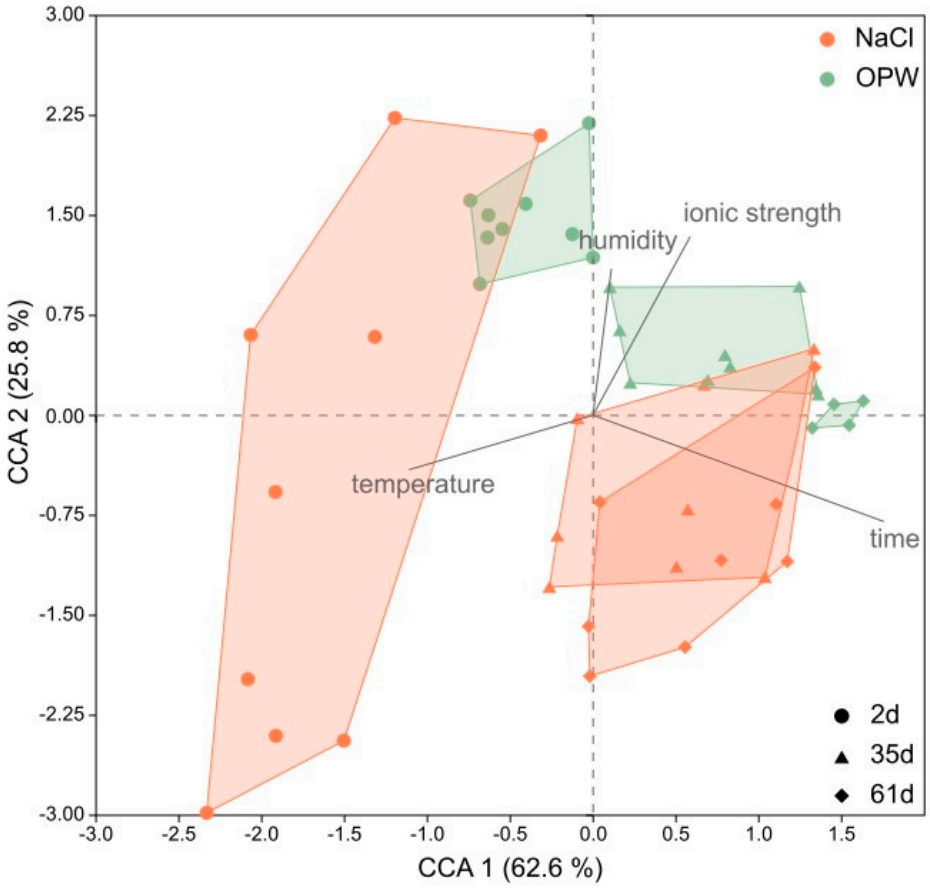


**Figure 5.** Canonical Correspondence Analysis (CCA) of XRD spectra of bentonite MX-80. Each cluster represents one sample analysed at different temperatures (27, 55, 80 °C) and relative humidity (0, 50, 80%). Dots represent samples after 2 days, triangles after 35 days and diamonds after 61 days of incubation in each solution (brown = NaCl, green = OPW).

## 4. Discussion

The present study aimed at investigating microbial as well as thermo-hydro-geochemical effects on the swelling capacity of MX-80 bentonite and, thus, on the integrity of bentonite as buffer material in a DGR.

### *4.1. Influence of Bentonite and Solution Composition on the Growth of S. bentonitica*

In this study, *S. bentonitica* was used as a model organism of the bentonite microbial population. It was grown at the optimal growth temperature of 28 °C in aerated mesocosms containing MX-80 bentonite and fluids of different ionic strength (salinity), but with NaCl concentrations well below the maximum, at which this organism is able to grow [44]. In fact, the single species was not able to survive under the control conditions without MX-80 in NaCl solutions. Slowly decreasing cell counts in NaCl and OPW in the presence of MX-80 as well as in OPW without MX-80 indicated that *S. bentonitica* may have benefited from metal nutrients or cations that were provided by minerals of MX-80 and the solution components of OPW. Metal nutrients and cations that can be provided by MX-80 bentonite include Si, Al, Ti, Fe, Mg, Ca, Na, K, P and S [41,42], while metal ions that were provided by OPW included Na, Ca, K, Mg and Sr. Given that *S. bentonitica* immediately died in NaCl solution, Na is not assumed to have a beneficial effect, leaving Ca, K and/or Mg as metal nutrient(s) that may have aided *S. bentonitica* in OPW and on MX-80. Ca, K and Mg belong to the interlayer cations in clay minerals which can be released most easily by cation exchange [37]. Although only Na and Ca are the typical interlayer cations of MX-80 bentonite, K and Mg were also present in each of the solutions with increasing concentrations over the course of

the experiment (Figure S3). Some cations such as Zn and Mg are universally essential for life and indispensable for nearly all aspects of metabolism [59,60]. Thus, the lack of Mg in NaCl without MX-80 supposedly caused the immediate death of *S. bentonitica*, while its presence in OPW and with MX-80 may have facilitated the survival of *S. bentonitica*.

However, *S. bentonitica* was not able to grow over prolonged periods of time in NaCl or OPW with MX-80. The lack of macronutrients such as nitrogen (N) in this experiment might have been a growth-limiting factor. N is one of the basic elements essential for the production of amino and nucleic acids [61]. While N in the form of nitrate can be used as an optional electron acceptor if oxygen is not available, ammonia/ammonium is an essential nutrient and energy source [62]. In a DGR, the introduction of N compounds during construction could have significant implications for the long-term safety of the stored nuclear waste, as ammonium or nitrate may increase the microbial activity. Some minerals such as illite can provide N in the form of ammonium [63]. However, illite is not a major mineral in MX-80 bentonite [41,42] and thus the lack of N could have been the reason for the final death of *S. bentonitica* in this experiment. The addition of $NH_4Cl$ to the mesocosms, however, did not have any beneficial effect (Figure S5).

Clay minerals are known to adsorb organic matter through different interactions which may reduce its availability for microorganisms [37,64,65]. However, low molecular weight compounds such as acetate, which was added to the mesocosm as carbon source, may have not been susceptible to adsorption, as preferentially organic matter with high molecular weight is adsorbed [66]. As the acetate content of the mesocosms was determined in the fluid phase, it was supposedly available for microbial breakdown. Nonetheless, as adsorption is related with the ionic strength of the surrounding solution and with pH [67–69], the low pH in NaCl and OPW (7.5–8.5; Figure S8) may have impeded the accessibility of acetate in those solutions. In general, the determined pH values are in the pH range in which *S. bentonitica* is able to grow [44] and are thus not assumed as limiting factors. The lower pH values of NaCl and OPW are rather favourable for *S. bentonitica* as a neutral pH is optimal for its growth [44].

In general, the lacking growth of *S. bentonitica* alone indicated that the incubation conditions were not favourable. Although *S. bentonitica* is able to grow aerobically under nutrient rich conditions, the agitation and aeration of the mesocosms seemed to be disadvantageous under nutrient limited conditions. In comparison, in the pre-cultures that were used to inoculate the mesocosms, acetate was depleted after 4 weeks (Figure S6) and *S. bentonitica* grew from $10^8$ or $10^9$ cells $mL^{-1}$ to about $10^{11}$ cells $mL^{-1}$ within 8 weeks (Figure S7). The pre-cultures were stored without agitation and were sampled at larger intervals than the mesocosms, creating microaerophilic conditions. *S. bentonitica* is capable of anaerobic respiration via nitrate reduction [44]. Denitrifying bacteria are mostly heterotrophic and often facultatively anaerobic with the ability to switch between oxygen and nitrate respiration depending on the environmental conditions [70]. Furthermore, the ability of closely related species such as *S. pavanii* and *S. maltophilia* to fix nitrogen [71,72] suggests that *S. bentonitica* may have the same capability.

In summary, the results indicate that despite the presence of a carbon and nitrogen source, and even though MX-80 supports the survival of microorganisms by potentially providing metal nutrients, *S. bentonitica* alone and under aerated conditions is not able to grow on MX-80 bentonite in moderate saline solutions.

### *4.2. Influence of S. bentonitica on the Swelling of MX-80*

As a consequence, similar XRD-patterns of bentonite incubated with and without *S. bentonitica* (Figure 3) strongly indicate that this bacterium did not alter montmorillonite and affect the swelling capacity of bentonite. This is underlined by a lack of significant changes in the clay elemental composition and the fluid (Figures S3 and S4). Similar to our observation, Perdrial et al. [42] observed a reduced growth of the bacterium *S. putrefaciens* and no chemical alteration of MX-80 bentonite, and assigned this to an excess of the monovalent cation $Na^+$ from the Na-montmorillonite. While divalent cations like $Ca^{2+}$

can facilitate bacterial adhesion and improve access to nutrients at the mineral surface, monovalent cations reduce the bridging effect between the negatively charged clay particles and the negatively charged bacteria [73]. This is supported by the fact that we could not observe an attachment or interaction of *S. bentonitica* cells with MX-80 bentonite using electron microscopy (Figure 1). Although *S. bentonitica* is known for biofilm formation [46,74], we found no evidence for biofilms on the surface of MX-80 bentonite under the given conditions in this study. In addition to excess $Na^+$, the access of the bacteria to mineral particles may be restricted due to the osmotic swelling of the Na-montmorillonite. The free movement and survival of bacteria can be significantly inhibited by the hydration of Na and the formation of a diffuse double layer, which leads to the formation of a gel [73,75,76]. We observed such a gel mainly in the NaCl mesocosm with MX-80 bentonite.

Although we could not observe an impact of *S. bentonitica* on the performance of MX-80 bentonite clay, this microbial species as part of a complex community or at different conditions in a natural environment may behave differently than the single species under laboratory conditions [77]. Recent studies showed that clays are inhabited by diverse microbial communities [27,78,79]. The depletion of oxygen several weeks after closing a DGR will inevitably change the metabolic and respiratory processes of this organism. Thus, we cannot exclude that *S. bentonitica* is able to affect the swelling capacity of MX-80 bentonite under conditions different from those tested in this study.

### *4.3. Influence of Hydro-Geochemical Parameters on the Swelling of MX-80 Bentonite*

#### 4.3.1. Swelling Capacity of Bentonite

In addition to the possible microbial impact on the swelling capacity of MX-80 bentonite, we investigated the effect of changing thermo-hydro-geochemical conditions such as temperature and humidity increase after contact to different solutions. The swelling capacity of bentonite is known to decrease with the increasing ionic strength of the surrounding solutions [22,80–87]. Such saline solutions cause an increase in electrolyte concentration inside the pore fluid and near the clay particle surfaces, diminishing the thickness of the double layer and the swelling potential [82]. After being in contact with solutions of different ionic strength, we found that an increased ionic strength, such as in NaCl and OPW solutions, impaired the swelling capability of bentonite. This was expressed by reduced shifts of the montmorillonite peak with increasing humidity, as well as a decreasing variance of sample clusters along the y-axis of a CCA (Figure 5). As only the water of the respective solutions was evaporated prior to XRD, the chemical components were still present and definitely affected the swelling behaviour. As a consequence, the contact of bentonite to saline pore waters such as Opalinus Clay pore water in a DGR with Opalinus Clay as the host rock is assumed to still impair the swelling of montmorillonite even though the solution may have already been evaporated.

The longer bentonite had contact to excess volumes of solution, the stronger the decrease in swelling was (Figures 5 and S2). Increasing concentrations primarily of Na, Ca and Mg over time in all three solutions (Figure S3) indicate that those typical interlayer cations [88] were leached from montmorillonite. However, they may also have their origin in the dissolution of the other accessory minerals, such as Ca from calcite or K from feldspars. Increasing element concentrations in the solutions could result in higher electrolyte concentrations around the clay particles and thereby diminish the thickness of the double layers. This is in line with the study of Herbert et al. [22] who showed that exchangeable Na, the sum of exchangeable cations and the total cation exchange capacity (CEC) decreased with reaction time in a solution. Higher concentrations of counterions between quasicrystals reduce the volume of aggregates and, thus, the swelling capacity of montmorillonite.

The ability of montmorillonite to incorporate various cations into the interlayer (CEC) is driven by an isomorphic substitution of cations in the octahedral sheets [89]. This leads to a development of a net negative charge of the silicate layers. Smectites are known for their irregular isomorphic substitution of cations, both in the octahedral as well as tetrahedral sheets. The consequential great variability of the negative layer charges is arbitrary, balanced by interlayer cations available from the surroundings [15]. Substitutions in the tetra- and octahedral sheets with cations of lower valence increase the layer charge, which is preferentially balanced by interlayer cations with higher valences. In the case of cations of the same valency, those with the higher atomic number are preferred [76]. The incorporation of divalent cations like $Ca^{2+}$ leads to a lower swelling potential as a consequence of ion–ion correlations [90,91]. Among all other cations, $K^+$ is believed to play a special role in contact with smectites. Even traces of $K^+$ ions, as can be observed at concentrations of ~20 and ~100 mg $L^{-1}$ in NaCl and OPW (Figure S3), respectively, are believed to cause mineral transformation that may cause a collapse of the interlayer space (e.g., [11,92,93] and degrade the bentonite performance. Kaufhold and Dohrmann (2010) [38] reported that a loss of swelling and water uptake due to $K^+$ was not related to illitisation, but rather to non-swelling collapsed $K^+$ smectite. Even though the salinity (ionic strength) of a solution affects the swelling (pressure) more than the type of the main cation in the exchange [22], both the ionic strength of the solution and the solution composition are factors controlling the swelling capacity. Thus, besides the slightly higher ionic strength of OPW compared to the NaCl solution, the presence of $K^+$ and/or the presence of divalent cations such as $Ca^{2+}$ and $Mg^{2+}$ may be the reason for the stronger reduction in the swelling capacity of MX-80 in OPW than in NaCl solution. This is supported from a study by Herbert (2008) [22], who found that the swelling pressure of bentonite decreased with the increasing salinity of a solution. They described a slight decrease in the swelling pressure in Opalinus Clay pore water with a minimum after one or two years in the solution.

#### 4.3.2. Reduced Peak Intensity

The strongly reduced diffraction peak intensity observed in the OPW samples made it difficult to evaluate the peak shifts and thus the swelling capacity of montmorillonite in OPW. The peak intensity was not only reduced in OPW but also in NaCl at the end of the experiment (Figure S2). The reduction both correlated with the time bentonite remained in the solution and the ionic strength of the solution. The extent of both factors influencing the decreasing peak intensity was concluded from the CCA (Figure 5). Shifts of the sample clusters, which reflect the decreasing peak intensity, mainly correlated with time and to a lesser extent with ionic strength.

The intensity of a diffraction peak is determined by a variety of factors. It can depend on the distribution of atoms in the crystal structure and it is therefore related to both the crystal structure and atom composition. However, Hofmann (2003) [15] found no indication for changes in the clay crystal structure caused by substitutions of the central cations in the tetrahedral or octahedral layers in saline solutions (NaCl, KCl, Q-solution). Hence, we assume that this was also not the reason for the decreasing peak intensity of MX-80 in NaCl and OPW solutions. Most likely, only the loosely bound interlayer cations were exchanged with changing solutions composition. Apart from several other factors like polarisation, multiplicity factor, Lorentz factor and absorption factor, the crystalline nature can influence the intensity of the scattered beam. If the crystalline nature (number of planes oriented in a particular direction) increases, the intensity increases. Hence, the observed decrease in XRD intensity might be due to a change in the crystal morphology. The valence of cations in solution as well as the layer charge of the smectites can influence the formation of aggregates. Bivalent cations in the solution can connect negatively charged layers and edges, resulting in the so called stair-step–cardhouse structure [94]. Bauer et al. [24] dedicated a decreasing peak intensity of Ceca smectite (a nearly pure montmorillonite) in acidic saline (NaCl and KCl) solutions to an increasing blocky morphology. They suggested that the flat smectite flakes cannot be piled to form a pseudo crystal on the glass sample slide with a

high coherent diffracting domain. The increasing disorder in the particle arrangement was concluded to be responsible for the decrease in XRD intensity as a function of time. Also, Bauer and Velde (1999) [13] observed a change in the smectite diffracting domain size in contact with KOH solution, which decreased with time. They assigned this observation to a change in the crystal shape. Thus, swelling is not only sensitive to the amount of non-swelling collapsed $K^+$ smectite layers or the presence of divalent cations, but also to the arrangement of smectite layers. This is supported by our observation of an increasing peak intensity after rinsing the samples with pure water. It suggests that changes in the morphology can be restored after removing the cations.

As a consequence, a reduced swelling of bentonite and changes in the morphology would reduce the integrity of bentonite as a technical barrier in a DGR and may facilitate microorganisms to better access the mineral particles as well as enable mineral alteration or migration. This would apply at least for uncompacted bentonite found at less densely packed interfacial environments and areas of disturbance, such as fractures and faults. This is exactly where fluid intrusion is likely to occur.

#### 4.3.3. Influence of Temperature

In addition to the ionic strength of a solution and the time bentonite remains in that solution, it could be shown that the temperature slightly reduced the swelling capacity (Figure 4). However, the experiment time was limited. It is possible that the influence of high temperature (>80 °C) will have a more significant effect on reducing the swelling capacity with longer exposure times. Since the early publications of Hofmann and Klemen [9], Greene-Kelly [10] and Weiss and Koch [11], it has been well accepted that at high temperatures, small cations like $Li^+$ can migrate through the tetrahedral sheet into the octahedral sheets, where they can neutralise the layer charge. This process leads to a decrease in the CEC, and therefore to a reduction in cations that can hydrate and cause swelling. The dehydration of the interlayer starts at temperatures between 70 and 109 °C [95] while a complete loss of intercrystalline swelling occurs at temperatures higher than 105–125 °C [9]. However, up to a temperature of 80 °C, properties like low permeability, water retention ability and self-healing capacity are usually maintained [96]

## 5. Conclusions

The safety of a DGR system has been well studied from a geological, chemical and physical point of view, but very few studies have investigated the combined effect of changing thermo-hydro-geochemical conditions and microbial processes on the safety of this disposal option. The multidisciplinary approach of this study aimed to evaluate the risk for transformation and alteration of bentonite clay minerals associated with microbial activity, changing pore fluid compositions and increasing temperature.

The study highlights that bentonite is affected by thermo-hydro-geochemical and microbial processes to different degrees. We show that the ionic strength of an invading solution and the solution composition are factors controlling the swelling behaviour of MX-80 bentonite. The swelling of uncompacted bentonite clay is severely reduced after exposure to moderately saline pore solutions and this effect increases with exposure time. Specifically, areas of disturbance, where uncompacted bentonite occurs and water intrusion is likely, are thus a safety risk for the integrity of a final repository. Further, we show that the activity of the model organism *S. bentonitica* under the conditions tested neither affect the swelling capacity significantly or alter the clay minerals.

Further work is needed to clarify whether this applies also to compacted bentonite and whether other microbial species or more complex communities under the conditions found in a repository have the potential to alter clay minerals and affect the swelling.

**Supplementary Materials:** The following supporting information can be downloaded at: https://www.mdpi.com/article/10.3390/applmicrobiol4030074/s1, Result S1: Bacterial growth with bentonite in $H_2O$; Result S2: Swelling behaviour of bentonite in $H_2O$; Figure S1: XRD spectra of bentonite MX-80 before and after sterilisation via electron beam irradiation; Figure S2: XRD spectra of MX-80 after 2, 35 and 61 d of incubation in $H_2O$, NaCl or OPW solutions, and after washing with ultrapure water; Figure S3: Element composition of the solutions $H_2O$, NaCl and OPW determined after 7, 35 and 61 days of contact with MX-80 bentonite; Figure S4: Element composition of MX-80 bentonite after 7, 35 and 61 days in $H_2O$, NaCl and OPW; Figure S5: Growth of *S. bentonitica* determined as CFU ml-1 in different solutions with and without the addition of MX-80 bentonite. All cultures were supplemented with NH4Cl as additional N-source; Figure S6: Acetate concentrations of $H_2O$, NaCl and OPW determined after 4 weeks in the initial solutions used for the batch experiments, in the control containing MX-80 but no S. bentonitica (+MX-80), in the pre-cultures used to inoculate the mesocosms (+S.b.) and in the experimental mesocosms containing S. bentonitica and MX-80 bentonite (+S.b. + MX-80); Figure S7: Growth of S. bentonitica determined as CFU ml-1 in different solutions without MX-80 bentonite, incubated at room temperature, without agitation and aeration; Figure S8: pH of the sterile filtered initial solutions used for the microcosms, pre-cultures that were not agitated, microcosms containing MX-80 and microcosms containing *S. bentonitica* and MX-80 after 69 days; Table S1: $d_{001}$ values of montmorillonite after exposure to NaCl and OPW solutions in presence or absence of bacteria determined at different temperatures and relative humidity. Table S2: Pairwise PerMANOVA used to analyse the difference in XRD-spectra of MX-80 incubated with (Bac) and without (NC) bacteria in $H_2O$, NaCl and OPW, Table S3: Calculation of the molar ionic strength I of the solutions $H_2O$, NaCl and OPW; Table S4: Mantel test of different factors controlling the peak position and intensity of MX80 bentonite in solutions of different ionic strength [97,98].

**Author Contributions:** Conceptualisation, J.M., A.M.S. and D.W.; methodology J.M., S.G. and M.B.; formal analysis, J.M. and A.M.S.; investigation, J.M. and A.M.S.; visualisation, J.M. and A.M.S.; data curation, A.M.S. and J.M.; writing—original draft preparation, J.M.; writing—review and editing, A.M.S., D.W. and S.G.; project administration, A.M.S. and D.W. All authors have read and agreed to the published version of the manuscript.

**Funding:** This work was supported by the German Federal Ministry of Education and Research (BMBF, Grant 02NUK053) and the Helmholtz Association (Grant SO-093).

**Data Availability Statement:** All data used in this study are freely available under the Creative Commons Attribution 4.0 International (CC BY 4.0) open access licence at GFZ data services [49].

**Acknowledgments:** We would like to thank the interdisciplinary team of the BMBF research project "iCross: integrity of nuclear waste repository systems—cross-scale system understanding and analysis", especially Michael Kühn (GFZ), for logistic support and coordination, as well as the BMBF for their generous support. The authors are thankful to thank Matthias Schmidt (UFZ) and for the use of the scanning electron microscope at the Centre for Chemical Microscopy (ProVIS) at UFZ Leipzig, which is supported by European Regional Development Funds (EFRE-Europe funds Saxony) and the Helmholtz Association. We would further like to thank Kristin Günther and Andrea Vieth-Hillebrandt for determining the acetate concentration.

**Conflicts of Interest:** The authors declare no conflicts of interest.

## References

1. Kim, J.S.; Kwon, S.K.; Sanchez, M.; Cho, G.C. Geological storage of high level nuclear waste. *KSCE J. Civ. Eng.* **2011**, *15*, 721–737. [CrossRef]
2. Grambow, B. Geological disposal of radioactive waste in Clay. *Elements* **2016**, *12*, 239–245. [CrossRef]
3. Bors, J.; Dultz, S.; Riebe, B. Retention of radionuclides by organophilic bentonite. *Eng. Geol.* **1999**, *54*, 195–206. [CrossRef]
4. Kozai, N. Sorption characteristics of americium on buffer material. In *Progress Report on Safety Research on Radioactive Waste Management for the Period April 1996 to March 1998*; Ohnuki, T., Muraoka, S., Banba, T., Eds.; Japan Atomic Energy Research Institute: Ibaraki, Japan, 1998; pp. 21–25.
5. Keto, P. *Natural Clays as Backfilling Materials in Different Backfilling Concepts*; Posiva Oy: Eurajoki, Finland, 2004.
6. Stroes-Gascoyne, S.; Hamon, C.J.; Maak, P.; Russell, S. The effects of the physical properties of highly compacted smectitic clay (bentonite) on the culturability of indigenous microorganisms. *Appl. Clay Sci.* **2010**, *47*, 155–162. [CrossRef]

7. Rutqvist, J.; Zheng, L.; Chen, F.; Liu, H.H.; Birkholzer, J. Modeling of coupled thermo-hydro-mechanical processes with links to geochemistry associated with bentonite-backfilled repository tunnels in clay formations. *Rock Mech. Rock Eng.* **2014**, *47*, 167–186. [CrossRef]
8. Delage, P.; Cui, Y.J.; Tang, A. Clays in radioactive waste disposal Clays in radioactive waste disposal. *J. Rock Mech. Geotech. Eng.* **2010**, *2*, 111–123. [CrossRef]
9. Hofmann, U.; Klemen, R. Verlust der Austauschfähigkeit von Lithiumionen an Bentonit durch Erhitzung. *Z. Anorg. Chem.* **1950**, *262*, 95–99. [CrossRef]
10. Greene-Kelly, K. Irreversible dehydration in montmorillonite, part II. *Clay Miner. Bull.* **1953**, *2*, 52–56. [CrossRef]
11. Weiss, A.; Koch, G. Über einen Zusammenhang zwischen dem Verlust des innerkristallinen Quellungsvermögens beim Erhitzen und dem Schichtaufbau bei glimmerartigen Schichtsilikaten. *Z. Naturforschung B* **1961**, *16*, 68–69. [CrossRef]
12. Gates, W.P.; Bouazza, A.; Jock Churchman, G. Bentonite clay keeps pollutants at bay. *Elements* **2009**, *5*, 105–110. [CrossRef]
13. Bauer, A.; Velde, B. Smectite transformation in high molar KOH solutions. *Clay Miner.* **1999**, *32*, 259–273. [CrossRef]
14. Herbert, H.-J.; Kasbohm, J.; Moog, H.C.; Henning, K.H. Long-term behaviour of the Wyoming bentonite MX-80 in high saline solutions. *Appl. Clay Sci.* **2004**, *26*, 275–291. [CrossRef]
15. Hofmann, H. Einfluss Konzentrierter Salzlösungen auf die Physiko-Chemischen Eigenschaften Quellfähiger Tonminerale: Konsequenzen für den Einsatz von Bentonit als Versatzmaterial in Einem Endlager für Schwach- und Mittelradioaktive Abfälle in Salzformationen. Ph.D. Thesis, University Heidelberg, Heidelberg, Germany, 2003.
16. Hofmann, H.; Bauer, A.; Warr, L.N. Behavior of smectite in strong salt brines under conditions relevant to the disposal of low- to medium-grade nuclear waste. *Clays Clay Miner.* **2004**, *52*, 14–24. [CrossRef]
17. Kasbohm, J.; Pusch, R.; Henning, K.-H. Short Term Experiments with Different Bentonites in Saline Solutions. In *Berichte der DTTG*; Nüesch, R., Emmerich, K., Eds.; Karlsruhe1432-7007; Deutsche Ton- und Tonmineralgruppe e.V.: Karlsruhe, Genmany, 2004; p. 47.
18. Suzuki, S.; Sazarashi, M.; Akimoto, T.; Haginuma, M.; Suzuki, K. A study of the mineralogical alteration of bentonite in saline water. *Appl. Clay Sci.* **2008**, *41*, 190–198. [CrossRef]
19. Kaufhold, S.; Dohrmann, R. Stability of bentonites in salt solutions III—Calcium hydroxide. *Appl. Clay Sci.* **2011**, *51*, 300–307. [CrossRef]
20. Stober, I.; Bucher, K. Origin of salinity of deep groundwater in crystalline rocks. *Terra Nov.* **2002**, *11*, 181–185. [CrossRef]
21. Pearson, F.J.; Arcos, D.; Bath, A.; Boisson, J.Y.; Fernández, A.M.; Gäbler, H.E.; Gaucher, E.; Gautschi, A.; Griffault, L.; Hernán, P.; et al. *Mont Terri Project—Geochemistry of Water in the Opalinus Clay Formation at the Mont Terri Rock Laboratory*; Federal Office for Water and Geology: Bern, Switzerland, 2003.
22. Herbert, H.J.; Kasbohm, J.; Sprenger, H.; Fernández, A.M.; Reichelt, C. Swelling pressures of MX-80 bentonite in solutions of different ionic strength. *Phys. Chem. Earth* **2008**, *33*, S327–S342. [CrossRef]
23. Adamcova, J.; Hanusova, I.; Ponavic, M.; Prikryl, R. Alteration processes in bentonites. In *Book of Abstracts of 18th Clay Conference in Czech Republic*; Stastny, M., Ed.; Czech National Clay Group: Prague, Czech Republic, 2008; p. 19.
24. Bauer, A.; Schafer, T.; Dohrmann, R.; Hoffmann, H.; Kim, J.I. Smectite stability in acid salt solutions and the fate of Eu, Th and U in solution. *Clay Miner.* **2001**, *36*, 93–103. [CrossRef]
25. Ferrage, E.; Lanson, B.; Sakharov, B.A.; Drits, V.A. Investigation of smectite hydration properties by modeling experimental X-ray diffraction patterns: Part I: Montmorillonite hydration properties. *Am. Mineral.* **2005**, *90*, 1358–1374. [CrossRef]
26. Kaufhold, S.; Dohrmann, R. Stability of bentonites in salt solutions I sodium chloride. *Appl. Clay Sci.* **2009**, *45*, 171–177. [CrossRef]
27. Lopez-Fernandez, M.; Cherkouk, A.; Vilchez-Vargas, R.; Jauregui, R.; Pieper, D.; Boon, N.; Sanchez-Castro, I.; Merroun, M.L. Bacterial Diversity in Bentonites, Engineered Barrier for Deep Geological Disposal of Radioactive Wastes. *Microb. Ecol.* **2015**, *70*, 922–935. [CrossRef]
28. Chapelle, F.H. *Ground-Water Microbiology and Geochemistry*; John Wiley & Sons: Hoboken, NJ, USA, 1993.
29. Brown, A.D. *Microbial Water Stress Physiology. Principles and Perspectives*; John Wiley & Sons: Hoboken, NJ, USA, 1990.
30. Courdouan-Metz, A. Nature and Reactivity of Dissolved Organic Matter in Clay Formations Evaluated for the Storage of Radioactive Waste. Ph.D. Thesis, Swiss Federal Institute of Technology in Zurich, Zurich, Switzerland, 2008.
31. Courdouan, A.; Christl, I.; Wersin, P.; Kretzschmar, R. Nature and reactivity of dissolved organic matter in the Opalinus Clay and Callovo-Oxfordian Formations. In Proceedings of the Clays in Natural and Engineered Barriers for Radioactive Waste Confinement, Lille, France, 17–20 September 2007.
32. Leupin, O.X.; Bernier-Latmani, R.; Bagnoud, A.; Moors, H.; Leys, N.; Wouters, K.; Stroes-Gascoyne, S. Fifteen years of microbiological investigation in Opalinus Clay at the Mont Terri rock laboratory (Switzerland). *Swiss J. Geosci.* **2017**, *110*, 343–354. [CrossRef]
33. Ehrlich, H.L. Microbes as geologic agents: Their role in mineral formation. *Geomicrobiol. J.* **1999**, *16*, 135–153. [CrossRef]
34. Gorshkov, A.I.; Drits, V.A.; Dubinina, G.A.; Bogdanova, O.A.; Sivtsov, A.V. The role of bacterial activity in the formation of hydrothermal Fe–Mn-formations in the northern part of the Lau Basin (south-western part of the Pacific Ocean). *Izv. Akad. Nauk Seriya Geol.* **1992**, *9*, 84–93.
35. Kawano, M.; Tomita, K. Microbial biomineralization in weathered volcanic ash deposit and formation of biogenic minerals by experimental incubation. *Am. Mineral.* **2001**, *86*, 400–410. [CrossRef]

36. Kohler, B.; Singer, A.; Stoffers, P. Biogenic nontronite from marine white smoker chimneys. *Clays Clay Miner.* **1994**, *42*, 689–701. [CrossRef]
37. Cuadros, J. Clay minerals interaction with microorganisms: A review. *Clay Miner.* **2017**, *52*, 235–261. [CrossRef]
38. Kaufhold, S.; Dohrmann, R. Stability of bentonites in salt solutions II. Potassium chloride solution—Initial step of illitization? *Appl. Clay Sci.* **2010**, *49*, 98–107. [CrossRef]
39. He, Y.; Ye, W.M.; Chen, Y.G.; Cui, Y.J. Effects of K + solutions on swelling behavior of compacted GMZ bentonite. *Eng. Geol.* **2019**, *249*, 241–248. [CrossRef]
40. Xiang, G.; Ye, W.; Xu, Y.; Jalal, F.E. Swelling deformation of Na-bentonite in solutions containing different cations. *Eng. Geol.* **2020**, *277*, 105757. [CrossRef]
41. Sauzeat, E.; Villiéras, T.F.; François, M.; Pelletier, M.; Barrés, O.; Yvon, J.; Guillaume, D.; Dubbessy, J.; Pfeiffert, C.; Ruck, R.; et al. Caractérisation minéralogique, cristallochimique et texturale de l'argile MX-80. *Rapport ANDRA No CRP0ENG* **2001**, 01–001.
42. Perdrial, J.N.; Warr, L.N.; Perdrial, N.; Lett, M.C.; Elsass, F. Interaction between smectite and bacteria: Implications for bentonite as backfill material in the disposal of nuclear waste. *Chem. Geol.* **2009**, *34*, 281–294. [CrossRef]
43. López-Fernández, M.; Fernández-Sanfrancisco, O.; Moreno-García, A.; Martín-Sánchez, I.; Sánchez-Castro, I.; Merroun, M.L. Microbial communities in bentonite formations and their interactions with uranium. *Appl. Geochem.* **2014**, *49*, 77–86. [CrossRef]
44. Sánchez-Castro, I.; Ruiz-Fresneda, M.A.; Bakkali, M.; Kämpfer, P.; Glaeser, S.P.; Busse, H.J.; López-Fernández, M.; Martínez-Rodríguez, P.; Merroun, M.L. Stenotrophomonas bentonitica sp. nov., isolated from bentonite formations. *Int. J. Syst. Evol. Microbiol.* **2017**, *67*, 2779–2786. [CrossRef] [PubMed]
45. Ruiz Fresneda, M.A.; Delgado Martín, J.; Gómez Bolívar, J.; Fernández Cantos, M.V.; Bosch-Estévez, G.; Martínez Moreno, M.F.; Merroun, M.L. Green synthesis and biotransformation of amorphous Se nanospheres to trigonal 1D Se nanostructures: Impact on Se mobility within the concept of radioactive waste disposal. *Environ. Sci. Nano* **2018**, *5*, 2103–2116. [CrossRef]
46. Ruiz-Fresneda, M.A.; Lopez-Fernandez, M.; Martinez-Moreno, M.F.; Cherkouk, A.; Ju-Nam, Y.; Ojeda, J.J.; Moll, H.; Merroun, M.L. Molecular Binding of EuIII/CmIIIby S tenotrophomonas bentonitica and Its Impact on the Safety of Future Geodisposal of Radioactive Waste. *Environ. Sci. Technol.* **2020**, *54*, 15180–15190. [CrossRef]
47. Joseph, C.; Schmeide, K.; Sachs, S.; Brendler, V.; Geipel, G.; Bernhard, G. Sorption of uranium(VI) onto Opalinus Clay in the absence and presence of humic acid in Opalinus Clay pore water. *Chem. Geol.* **2011**, *284*, 240–250. [CrossRef]
48. Pearson, F.J. *Opalinus Clay Experimental Water: A1Type, Version 980318*; Paul Scherrer Institut: Villigen, Switzerland, 1998.
49. Schleicher, A.M.; Mitzscherling, J.; Bonitz, M.; Genderjahn, S.; Wagner, D. Mineralogical, geochemical and microbial dataset for assessing the impact of *S. bentonitica* in different solutions on the performance of bentonite clay at changing thermo-hydro-chemical conditions. *GFZ Data Serv.* **2024**. [CrossRef]
50. Courdouan, A.; Christl, I.; Meylan, S.; Wersin, P.; Kretzschmar, R. Characterization of dissolved organic matter in anoxic rock extracts and in situ pore water of the Opalinus Clay. *Appl. Geochem.* **2007**, *22*, 2926–2939. [CrossRef]
51. Miles, A.A.; Misra, S.S.; Irwin, J.O. The estimation of the bactericidal power of the blood. *J. Hyg.* **1938**, *38*, 732–749. [CrossRef]
52. Hammer, Ø.; Harper, D.A.T.; Ryan, P.D. PAST: Paleontological Statistics Software Package for Education and Data Analysis. *Palaeontol. Electron.* **2001**, *4*, 1–9.
53. McNaught, A.D.; Wilkinson, A. *IUPAC. Compendium of Chemical Terminology*, 2nd ed.; Blackwell Scientific Publications: Oxford, UK, 1997. [CrossRef]
54. Eberl, D.D.; Hower, J. The hdrothermal transformation of sodium and potassium smectite into mixed-layer clay. *Clays Clay Miner.* **1977**, *25*, 215–227. [CrossRef]
55. Inoue, A. Potassium fixation by clay minerals during hydrothermal treatment. *Clays Clay Miner.* **1983**, *31*, 81–91. [CrossRef]
56. Komareni, S.; White, W.B. Hydrothermal reaction of strontium and transuranic simulator elements with clay minerals, zeolites and shales. *Clays Clay Miner.* **1983**, *31*, 113–121. [CrossRef]
57. Kasbohm, J.; Venz, C.; Henning, K.-H.; Herbert, H.-J. Zu Aspekten einer Lang- zeitsicherheit von Bentonit in hochsalinaren Lösungen. In *Berichte der Deutschen Ton- und Tonmineralgruppe e.V.-Beiträge zur Jahrestagung*; Stengele, H., Plötze, M., Eds.; ETH Zürich: Zurich, Switzerland, 2000; pp. 158–170.
58. Finsterle, S.; Muller, R.A.; Baltzer, R.; Payer, J.; Rector, J.W. Thermal evolution near heat-generating nuclear waste canisters disposed in horizontal drillholes. *Energies* **2019**, *12*, 596. [CrossRef]
59. Merchant, S.S.; Helmann, J.D. Elemental Economy. Microbial Strategies for Optimizing Growth in the Face of Nutrient Limitation. In *Advances in Microbial Physiology*, 1st ed.; Elsevier Ltd.: Amsterdam, The Netherlands, 2012. [CrossRef]
60. Perez Rodriguez, J.L.; Carretero, M.I.; Maqueda, C. Behaviour of sepiolite, vermiculite and montmorillonite as supports in anaerobic digesters. *Appl. Clay Sci.* **1989**, *4*, 69–82. [CrossRef]
61. Bothe, H.; Ferguson, S.; Newton, W.E. *Biology of the Nitrogen Cycle*; Elsevier Science: Amsterdam, The Netherlands, 2007.
62. Kutvonen, H.; Rajala, P.; Carpén, L.; Bomberg, M. Nitrate and ammonia as nitrogen sources for deep subsurface microorganisms. *Front. Microbiol.* **2015**, *6*, 1079. [CrossRef]
63. Landeweert, R.; Hoffland, E.; Finlay, R.D.; Kuyper, T.W.; van Breemen, N. Linking plants to rocks: Ectomycorrhizal fungi mobilize nutrients from minerals. *Trends Ecol. Evol.* **2001**, *16*, 248–254. [CrossRef]
64. Kieft, T.L. Size matters: Dwarf cells in soil and subsurface terrestrial environments. In *Non-Culturable Microorganisms in the Environment*; Colwell, R.R., Grimes, D.J., Eds.; ASM Press: Washington, DC, USA, 2000; pp. 19–46.

65. Curry, K.J.; Bennett, R.H.; Mayer, L.M.; Curry, A.; Abril, M.; Biesiot, P.M.; Hulbert, M.H. Direct visualization of clay microfabric signatures driving organic matter preservation in fine-grained sediment. *Geochim. Cosmochim. Acta* **2007**, *71*, 1709–1720. [CrossRef]
66. Chorover, J.; Amistadi, M.K. Reaction of forest floor organic matter at goethite, birnessite and smectite surfaces. *Geochim. Cosmochim. Acta* **2001**, *65*, 95–109. [CrossRef]
67. Murphy, E.M.; Zachara, J.M.; Smith, S.C.; Phillips, J.L.; Wietsma, T.W. Interaction of hydrophobic organic compounds with mineral-bound humic substances. *Environ. Sci. Technol.* **1994**, *28*, 1291–1299. [CrossRef] [PubMed]
68. Schlautman, M.A.; Morgan, J.J. Adsorption of aquatic humic substances on colloidal-size aluminum oxide particles: Influence of solution chemistry. *Geochim. Cosmochim. Acta* **1994**, *58*, 4293–4303. [CrossRef]
69. Arnarson, T.S.; Keil, R.G. The role of reactive surface sites and complexation by humic acids in the interaction of clay mineral and iron oxide particles. *Mar. Chem.* **2000**, *71*, 309–320. [CrossRef]
70. Luque-Almagro, V.M.; Gates, A.J.; Moreno-Vivián, C.; Ferguson, S.J.; Richardson, D.J.; Roldan, M.D. Bacterial nitrate assimilation: Gene distribution and regulation. *Biochem. Soc. Trans.* **2011**, *39*, 1838–1843. [CrossRef] [PubMed]
71. Bashandy, S.R.; Abd-Alla, M.H.; Dawood, M.F.A. Alleviation of the toxicity of oily wastewater to canola plants by the N2-fixing, aromatic hydrocarbon biodegrading bacterium Stenotrophomonas maltophilia-SR1. *Appl. Soil Ecol.* **2020**, *154*, 103654. [CrossRef]
72. Ramos, P.L.; Van Trappen, S.; Thompson, F.L.; Rocha, R.C.S.; Barbosa, H.R.; de Vos, P.; Moreira-Filho, C.A. Screening for endophytic nitrogen-fixing bacteria in Brazilian sugar cane varieties used in organic farming and description of stenotrophomonas Pavanii sp. nov. *Int. J. Syst. Evol. Microbiol.* **2011**, *61*, 926–931. [CrossRef]
73. Simoni, S.F.; Bosma, T.N.P.; Harms, H.; Zehnder, A.J.B. Bivalent Cations Increase Both the Subpopulation of Adhering Bacteria Sand Columns. *Environ. Sci. Technol.* **2000**, *34*, 1011–1017. [CrossRef]
74. Sánchez-Castro, I.; Bakkali, M.; Merroun, M.L. Draft genome sequence of Stenotrophomonas bentonitica BII-R7, a selenite-reducing bacterium isolated from Spanish bentonites. *Genome Announc.* **2017**, *5*, 7–9. [CrossRef]
75. MacEwan, D.M.C.; Wilson, M.J. Interlayer and intercalation complexes of clay minerals. In *Crystal Structure of Clay Minerals and their X-ray Identification*; Brindley, G.W., Brown, G., Eds.; Mineralogical Society: London, UK, 1980; pp. 197–242.
76. Lagaly, G. Reaktionen der Tonminerale. In *Tonminerale und Tone: Struktur, Eigenschaften und Einsatz in Industrie und Umwelt*; Jasmund, K., Lagaly, G., Eds.; Steinkopff Verlag: Darmstadt, Germany, 1993; pp. 89–167.
77. Wintermute, E.H.; Silver, P.A. Emergent cooperation in microbial metabolism. *Mol. Syst. Biol.* **2010**, *6*, 407. [CrossRef]
78. Boivin-Jahns, V.; Ruimy, R.; Bianchi, A.; Daumas, S.; Christen, R. Bacterial diversity in a deep-subsurface clay environment. *Appl. Environ. Microbiol.* **1996**, *62*, 3405–3412. [CrossRef]
79. Mitzscherling, J.; Genderjahn, S.; Schleicher, A.M.; Bartholomäus, A.; Kallmeyer, J.; Wagner, D. Clay-associated microbial communities and their relevance for a nuclear waste repository in the Opalinus Clay rock formation. *Microbiologyopen* **2023**, *12*, e1370. [CrossRef]
80. Suzuki, S.; Prayongphan, S.; Ichikawa, Y.; Chae, B.G. In situ observations of the swelling of bentonite aggregates in NaCl solution. *Appl. Clay Sci.* **2005**, *29*, 89–98. [CrossRef]
81. Pusch, R.; Karnland, O.; Hökmark, H. *GMM-A General Microstructural Model for Qualitative and Quantitative Studies on Smectite Clays*; Swedish Nuclear Fuel and Waste Management Co.: Stockholm, Sweden, 1990.
82. Castellanos, E.; Villar, M.V.; Romero, E.; Lloret, A.; Gens, A. Chemical impact on the hydro-mechanical behaviour of high-density FEBEX bentonite. *Phys. Chem. Earth* **2008**, *33*, S516–S526. [CrossRef]
83. Karnland, O.; Olsson, S.; Nilsson, U. *Mineralogy and Sealing Properties of Various Bentonites and Smectite-Rich Clay Materials*; TR-06-30; Swedish Nuclear Fuel and Waste Management Co.: Stockholm, Sweden, 2006; pp. 3–70.
84. Komine, H.; Yasuhara, K.; Murakami, S. Swelling characteristics of bentonites in artificial seawater. *Can. Geotech. J.* **2009**, *46*, 177–189. [CrossRef]
85. Siddiqua, S.; Blatz, J.; Siemens, G. Evaluation of the impact of pore fluid chemistry on the hydromechanical behaviour of clay-based sealing materials. *Can. Geotech. J.* **2011**, *48*, 199–213. [CrossRef]
86. Lee, J.O.; Lim, J.G.; Kang, I.M.; Sangki, K. Swelling pressures of compacted Ca-bentonite. *Eng. Geol.* **2012**, *129–130*, 20–26. [CrossRef]
87. Chun-Ming, Z.; Wei-Min, Y.; Yong-Gui, C.; Bao, C.; Yu-Jun, C. Influence of salt solutions on the swelling pressure and hydraulic conductivity of compacted GMZ01 bentonite. *Eng. Geol.* **2013**, *166*, 74–80. [CrossRef]
88. Sato, H. Quantification of exchangable cations in interlayer of Tsukinuno Sodium-Montmorillonite. *Mater. Res. Soc. Symp. Proc.* **2009**, *1193*, 2–7. [CrossRef]
89. Dohrmann, R.; Genske, D.; Karnland, O.; Kaufhold, S.; Kiviranta, L.; Olsson, S.; Plötze, M.; Sandén, T.; Sellin, P.; Svensson, D.; et al. Interlaboratory CEC and exchangeable cation study of bentonite buffer materials: I. Cu(II)-triethylenetetramine method. *Clays Clay Miner.* **2012**, *60*, 162–175. [CrossRef]
90. Segad, M.; Jönsson, B.; Åkesson, T.; Cabane, B. Ca/Na montmorillonite: Structure, forces and swelling properties. *Langmuir* **2010**, *26*, 5782–5790. [CrossRef]
91. Liu, L. Colloids and Surfaces A: Physicochemical and Engineering Aspects Prediction of swelling pressures of different types of bentonite in dilute solutions. *Colloids Surf. A Physicochem. Eng. Asp.* **2013**, *434*, 303–318. [CrossRef]
92. Push, R. *The Buffer and Backfill Handbook Part 1—Definitions, Basic Relationships, and Laboratory Methods*; SKB Technical Report SKB-TR-02-20; Swedish Nuclear Fuel and Waste Management Co.: Stockholm, Sweden, 2002.

93. Push, R. *The Buffer and Backfill Handbook Part 2—Materials and Techniques*; SKB Technical Report SKB-TR-02-12; Swedish Nuclear Fuel and Waste Management Co.: Stockholm, Sweden, 2002.
94. O'Brien Fabric of kaolinite and illite floccules. *Clays Clay Miner.* **1971**, *19*, 353–359. [CrossRef]
95. Schleicher, A.M.; Warr, L.N.; Van Der Pluijm, B.A. On the origin of mixed-layered clay minerals from the San Andreas Fault at 2.5–3 km vertical depth (SAFOD drillhole at Parkfield, California). *Contrib. Mineral. Petrol.* **2009**, *157*, 173–187. [CrossRef]
96. Villar, M.V.; Lloret, A. Influence of temperature on the hydro-mechanical behaviour of a compacted bentonite. *Appl. Clay Sci.* **2004**, *26*, 337–350. [CrossRef]
97. Colten-Bradley, V.A. Role of Pressure in Smectite Dehydration—Effects on Geopressure and Smectite-To-Illite Transformation. *Am. Assoc. Pet. Geol. Bull.* **1987**, *71*, 1414–1427. [CrossRef]
98. Ikari, M.J.; Saffer, D.M.; Marone, C. Effect of hydration state on the frictional properties of montmorillonite-based fault gouge. *J. Geophys. Res. Solid Earth.* **2007**, *112*, 1–12. [CrossRef]